

G. BAUDIN<sup>+</sup> and M. ROBERT<sup>+</sup>

ABSTRACT

In a first part the crack growth model developed at ONERA is described. This model mainly consists of two relations, the first one relating the crack growth rate to the effective SIF but using the evolutive propagation threshold concept, the second one defining the threshold evolution from two experimental functions.

Adapted to crack growth calculation under aeronautical type loadings like standard spectra, the model is used in a second part for predicting numerous life-times resulting of tests with various conditions in particular various loadings. The comparison between predictions and tests is considered as good.

INTRODUCTION

The prediction of fatigue crack growth under variable loading is still a problem widely studied in aeronautics. As is known the presence of cracks in certain aircraft structures is admitted if aircraft designers are able to predict their evolution under service loading. The first crack growth models accounting for loads interaction effect were those of Wheeler (1) and Willenborg (2) often used till now in in-house procedures of aircraft manufacturers. More recently, works of Newman (3), Johnson (4), Rudd and Engle (5), Chang et al (6), Schivje (7), De Koning (8) have to be mentioned among others.

Concerning studies carried out at ONERA on this point, Pellas et al (9) also proposed a crack growth model taking into account the history effect due to a variable loading and based on the concept of propagation threshold, apparently similar to the crack opening concept of Elber (10). Owing to difficulties of use, the authors (11) presented a new simplified version of the model, made valid for standard aeronautical loadings thanks to an adjustable loading parameter. In this paper the last developments of this model are described, namely the accounting for thickness effect and the determination of the loading parameter of any loading by a simple method. Using the model we present lastly a comparison between fatigue crack growth life-time predictions and corresponding tests. More of 70 results are reviewed dealing with various condition such as specimen type, alloys, thicknesses, spectra and load levels.

+ ONERA - Office National d'Etudes et de Recherches Aérospatiales - BP 72 -  
92322 Chatillon Cedex - France

## DESCRIPTION OF THE CRACK GROWTH PREDICTION MODEL

In these first part the main features of the model are recalled.

### Propagation threshold concept

The model is based on the notion of evolutive propagation threshold defined in the following way (fig 1). First a crack grows under a variable loading expressed, for example, in term of stress intensity factor (SIF). This loading is stropped at a minimum value  $K_m$ , then a constant amplitude loading ( $K_M$ ,  $K_m$ ) is applied. Experiments show that it is always possible to determine a limit value  $K_S$  such that :

if  $K_M > K_S$  then the crack continues to grow  
if  $K_M < K_S$  then the crack arrests.

We thus determined a threshold loading ( $K_S$ ,  $K_m$ ) where  $K_S$  is, in particular, connected to  $K_m$ . It would be interesting to compare the two concepts of propagation threshold force and crack opening force proposed by Elber (10), but we say simply that they apparently correspond to the same physical process.

### Threshold loading measurement for basic loadings

Pellas et al (12) used the above procedure in the two basic cases : constant amplitude (CA) loading and CA loading ended by an overload.

Overload case. The parameter  $R$  is defined as the ratio of minimum level  $K_m$  following the overload over the overload level  $K_{MO}$ . For every value of  $R$ , the limit loading ( $K_S$ ,  $K_m$ ) is measured. Plotting the  $K_S$  values normalized by  $K_{MO}$  versus the parameter  $R$ , an experimental curve is determined and called "function  $f_1$ " (see fig 2).

It is worth to note that experiments show two facts : first  $f_1$  is practically independent of the level  $K_{MO}$  and secondly, the loading before the overload has a very light influence on the level  $K_S$ , provided that  $K_{MO}$  be large compared to the maximum level of the prior loading. This fact is well known : after an overload the new loading history is mainly the one due to the overload. Finally the threshold level after one overload is given by :

$$K_S = K_{MO} \times f_1(R) \quad (1)$$

$$\text{with } R = K_m / K_{MO}$$

Constant amplitude case. A second "function  $f_2$ " can be measured in the similar manner in this situation (Fig 3). As  $f_1$ ,  $f_2$  does not depend significantly on the  $K_M$  level. Besides the  $K_S$  level is practically unaffected by variation of minimum level of the loading before the last maximum. And then for CA loading ( $K_M$ ,  $K_m$ ) the threshold level is defined as :

$$K_S = K_M \times f_2(R) \quad (2)$$

$$\text{with } R = K_m / K_M$$

It must be understood that the use of these two experimental functions constitute one of the main features of the ONERA model and interesting comments about them can be added :

- the two functions are considered as intrinsic to the material at given thickness.

- if one compares  $f_1$  to  $f_2$ ,  $f_2$  is higher than  $f_1$  for a given  $R$  value. The two functions constitute the lower and upper limits of the relative threshold level in the multiple overloads case. In a slight different manner, it can be concluded that after an arbitrary loading ended by a highest value  $K_M$  followed by a minimum value  $K_m$ , the threshold level  $K_S$  stands between two limits :

$$K_M \times f_1(R) < K_S < K_M \times f_2(R) \quad (3)$$

$$\text{with } R = K_m / K_M$$

- the function  $f_2$  makes it possible the definition of a crack growth model valid for CA loading and taking into account the  $R$  effect.

- when two materials are comparatively tested, the one giving highest function  $f_1$  is the more sensitive regarding the retardation effect due to overloads or variable loadings.

### Variable amplitude loading - Assumptions

In order to simplify the difficult problem of loads interaction which is of importance concerning crack growth rate, we make the following assumptions :

i - we consider that the mechanical history due to any variable loading can be expressed at the last cycle by three internal variables, to say

$K_S$  threshold SIF already mentioned

$K_{Meq}$  maximum equivalent SIF

$K_{meq}$  minimum equivalent SIF

The role of  $K_{Meq}$  and  $K_{meq}$  is respectively to memorize overloads and compressive loads effect.

ii- as a definition of  $K_{Meq}$  and  $K_{meq}$  we assume that the loading history of this variable loading is intermediate between the one due to an overload  $K_{Meq}$  followed by  $K_{meq}$  and the one due to a CA loading ( $K_{Meq}$ ,  $K_{meq}$ ). Therefore the threshold level lies between two values like in the expression 3 with  $K_{Meq}$  and  $K_{meq}$  instead  $K_M$  and  $K_m$ .

iii - for determining the position of the threshold level  $K_S$  we introduce now a weighting parameter  $\alpha$  between the two functions  $f_1$  and  $f_2$ . It is legitimate to think that  $\alpha$  varies from cycle to cycle during a variable loading but, unfortunately, it is difficult to establish a simple evolution law for it. That is why we propose to give  $\alpha$  a constant average value, this value being connected to the variable character of the considered loading. This procedure seems reasonable when the involved loading is a repeated sequence like aeronautical standard spectrum. Then  $\alpha$ , loading parameter, is considered to be representative of the type of the spectrum. Resulting of both its definition and an arbitrary choice,  $\alpha$  stands between two particular values :

$$\alpha = 0 \text{ for CA loading case}$$

$\alpha = 1$  for one overload case

### Formulation of the model

The model performs a cycle-by-cycle calculation of crack growth. When the cycle  $i$ , defined by the values  $KM_i$  and  $Km_i$ , is applied the increasing part, from  $KS_{i-1}$  up to  $KM_i$ , involves an increment of crack length  $\Delta a_i$  and a change of  $KMeq$ . Then the decreasing part down to  $Km_i$  entails variations of both  $KS$  and  $Kmeq$ . And so on for the following cycles (Fig 4).

In order to make clearer the constitutive formulations of the model we distinguish, among cycles pertaining to any loading, five types of cycle defined from the configuration of the three internal variables. On the fig. 5 the consequences of every type are summarized.

Crack growth formulation. This formulation, valid for type of cycle 3, 4 and 5, introduce an effective SIF in a classical manner by using the propagation threshold SIF instead of the opening SIF of Elber. The second part of the formulation relates the threshold SIF to  $KMeq$  with the need of  $f_1$ ,  $f_2$  and  $\alpha$ .

$$\Delta a_i = C (KM_i - KS_{(i-1)})^n \quad (4)$$

$$KS_i = KMeq_i [af_1(Req_i) + (\alpha-1).f_2(Req_i)] \quad (5)$$

$$\text{with } Req_i = Kmeq_i / KMeq_i$$

$$(\text{if } KS_i < Km_i \text{ then } KS_i = Km_i)$$

### Evolution of $KMeq$

In the paper mentionned (11)  $KMeq$  is defined as the SIF giving the actual plastic zone size  $\rho$  at the crack tip through the Irwin's formula in plane stress case :

$$\rho = \frac{1}{\pi} \left( \frac{KMeq}{\sigma_{YS}} \right)^2 \quad (6)$$

$$\text{and } KMeq = \sigma_{YS} \sqrt{\pi \cdot \rho} \quad (7)$$

For applying the model with thick specimen, the thickness  $e$  must be accounting for in the estimation of the plastic zone size. In this purpose we adopted a diagram of plastic zone shown on the Fig 6 which allows us to introduce a mean plastic zone size  $\rho_m$  defined from the plastic surface.

In this simple but qualitatively reasonable diagram we assume that first the plane stress-plane strain plastic zone sizes ratio equals 6 and secondly the plastic zone size decreases into the thickness following a  $45^\circ$  straight line. As shown, two situations (a or b) occur :

$$\text{a - } \rho < 0.6 e \text{ and } \rho_m = \frac{\rho}{6} \left( 1 + \frac{25}{6} \cdot \frac{\rho}{e} \right) \quad (8)$$

$$\text{b - } \rho > 0.6 e \text{ and } \rho_m = \rho - \frac{e}{4} \quad (9)$$

We consider now the evolution of  $\rho_m$  when the cycle  $i$  is applied. For the types of cycle 1, 2, 3 and 5 the plastic zone is unchanged or decreases because the crack grows :

$$\rho_m = \rho_m(i-1) - \Delta a_i \quad (10)$$

For the type 4, overload case, the plastic zone first increases when  $KM_i$  applies :

$$\rho_{OL} = \frac{1}{\pi} \left( \frac{KM_i}{\sigma_{YS}} \right)^2 \quad (11)$$

and  $\rho_{mOL}$  can be deduced through the relation 8 or 9 in using  $\rho_{OL}$  instead of  $\rho$ . Then  $\rho_{mOL}$  decreases because the crack grows :

$$\rho_{m_i} = \rho_{mOL} - \Delta a_i \quad (12)$$

For every type of cycle we have now to determine  $KMeq_i$  from  $\rho_{m_i}$  in accordance with the situation a or b. For that we introduce an equivalent plane stress plastic zone size  $\rho_{eq_i}$  by inversing relations 8 and 9 :

$$\text{a - } \rho_{eq_i} = 0.12 e \left[ \sqrt{1 + 0.01 \frac{\rho_{m_i}}{e}} - 1 \right] \quad (13)$$

$$\text{b - } \rho_{eq_i} = \rho_{m_i} + \frac{e}{4} \quad (14)$$

and finally :

$$KMeq_i = \sigma_{YS} \sqrt{\pi \cdot \rho_{eq_i}} \quad (15)$$

### Evolution of $Kmeq$

The analysis of numerous experimental results obtained in our laboratory led us to propose an evolution of  $Kmeq$  as follows :

for cycle type 1, obviously

$$Kmeq_i = Kmeq_{(i-1)} \quad (16)$$

for type 2,3 and 4

$$Kmeq_i = Km_i \quad (17)$$

For type 5 we have to establish a specific relationship. We propose in this paper a new formulation, close to the one of reference (11), but accounting for a thickness effect deduced from our observations :

$$Kmeq_i = Kmeq_{(i-1)} + \Delta Kmeq_i \quad (18)$$

$$\text{with } \Delta Kmeq_i = (Km_i - Kmeq_{(i-1)}) \cdot \left[ \frac{KM_i}{KMeq_i} \right]^B \quad (19)$$

This formula gives an intermediate result between the ones of relations 16 and 17, depending on the  $K_{Mi}$  level compared to the  $K_{Meqi}$  one. Lastly we take  $\beta$  as :

$$\beta = 2 + e/2 \quad (20)$$

where the thickness  $e$  is expressed in mm. Of course the choice of relations 19 and 20 is rather arbitrary and variations of them may occur in the future.

#### Determination of the loading parameter

From its definition the loading parameter  $\alpha$  stands between 0 for CA loading and 1 after one overload, but it is undefined for a variable loading. A first answer is given in reference (11) where  $\alpha$  was adjusted for matching with propagation tests under FALSTAFF and MINITWIST spectra. It was found respectively  $\alpha = 0.65$  and  $0.5$ . We propose now a simple method to determine  $\alpha$  for any loading sequence. Let be a sequence of  $N$  cycles with maximum  $M_i$  levels and the highest level Max, then  $\alpha$  is given by :

$$\alpha = 1 - \frac{1}{N \cdot \text{Max}} \cdot \sum_{i=1}^N M_i \quad (21)$$

This simple formula provides reasonable results for spectra involved in this paper, in particular for FALSTAFF and MINITWIST as it is shown later on table II.

#### Exemple of identification

The material data to be determined are the functions  $f_1$  and  $f_2$  and constants  $C$  and  $n$  (yield stress  $\sigma_{YS}$  is known). For 2024-T3, 2 mm. thick, the experimental determination of  $f_1$  is shown on Fig 8. For positive  $R$ , a straight line give a good representation of it. This means that the knowledge of  $R_1^C$  (critical overload ratio,  $R = 0$ , for which blocking effect occurs) allows an easy determination of  $f_1$ . This result is confirmed for all materials we tested. A second straight line completes the function  $f_1$  for negative  $R$ . Regarding  $f_2$ , the relationship on the Fig 8 matches well with experimental measurements when using  $R_2^C$  (critical high-low ratio,  $R = 0$ , which gives blocking effect in two levels test).

Crack growth constants are classically determined from CA tests with  $R = 0$  (Fig 7). Then  $C$  is easily related to the constant  $C_0$  of the Paris's law :

$$da/dN = C_0 \cdot K_M^n = C \cdot (K_M - K_S)^n \quad (22)$$

$$\text{with } K_S = K_M \cdot f_2(0)$$

$$\text{then } C = C_0 / [1 - f_2(0)]^n \quad (23)$$

It is worth to note that CA test results at  $R = 0$  added to the knowledge of  $f_2$  allow to establish a law accounting for  $R$  effect. Combining 22 and 23 it gives :

$$da/dN = C_0 \cdot K_M^n \left[ \frac{1 - f_2(R)}{1 - f_2(0)} \right]^n \quad (24)$$

In inverse order, CA test results at variable  $R$  allow to determine  $f_2(R)$  with the help of  $R_2^C$  or  $f_2(0)$ .

#### LIFE-TIME CALCULATIONS - COMPARISON WITH TESTS

The operational form of the crack growth model is a FORTRAN code. It was used to calculate and compare life-times of specimens tested under aeronautical type loadings. For this purpose the first step was collecting available experimental results.

#### Crack growth data-base

More of 70 distinct test results have been accounting for. Various conditions are met : specimen types, light alloys, thicknesses, civil and military aircraft spectra, load levels. A part of these results has been drawn from publications of Van der Linden (13), Salvetti et al. (14), Chang (15), Gunther and Goranson (16), Baudin et al. (17). Other sources are unpublished CEAT, Aerospatiale, ONERA reports.

Concerning spectra, all of them have an aeronautical origin. More precisely they are considered to be representative for the loads history of the wing root of aircraft. They consist of a serie of simulated flights. We distinguished two types of spectrum, military and civil ones. In order to show their particular variable character, Fig 10 and 11 represent flights pertaining respectively to standard military spectrum FALSTAFF and civil spectrum MINITWIST.

Regarding materials, all of them are light alloys widely used in aircraft industry. Thicknesses range from 1.6 mm. to 12 mm. and specimens are of CT and CCT types.

#### Material data

The constants used for calculations are summarized on the table I. In order to compare materials regarding crack growth rate, we took an unique mean value, 3, as slope of Paris's straight line. Then  $C_0$  is deduced from constant amplitude tests accompanying tests under spectrum loading.

Concerning functions  $f_1$  and  $f_2$  (or  $R_1^C$  and  $R_2^C$  ratios) results are not available for several materials. Therefore we only used 2024.T3 results for all of them. Of course this may be a source of error.

TABLE 1

MATERIEL	THICKNESS (mm)	YIELD STRESS (MPa)		(MPa, m)
- 2024 - T3	2.	340	3	$0.95 \cdot 10^{10}$
- 2024 - T3	1.62	340	3	0.83
- 2024 - T3*	2.	340	3	0.40
- 2024 - T351	10. and 12.	340	3	0.95
- 2214 - T651	10.	428	3	1.25
- 2219 - T851	6.35	360	3	1.14
- 7475 - T7351	10.	400	3	0.78

\* Specimens machined from a thick sheet.

Loading parameters

The loading parameters  $\alpha$  are calculated through the formula 21 and put on the table II for the 8 types of spectrum and their different versions.  $\alpha$  ranges from 0.42 to 0.70 with the trend to be higher for military spectra.

TABLE II

TYPE	ORIGIN	VERSION	
Military Aircraft Spectrum	FALSTAFF	Standard	0.68
		Reduced	0.62
		Troncated low (8)	0.67
		Red. and tronc.	0.59
	AMDBA	Base	0.52
		Troncated high	0.45
		Overload added	0.57
	SFM-GT4	Reference	0.70
		Prog. Blocks	0.64
		FALSTAFF type	0.68
	AS TM-STP 748	M 81	0.46
		M 84	0.51
		M 88	0.55
M 90		0.51	
Civil aircraft Spectrum	TWIST	Standard	0.52
		Troncated high (2.3)	0.46
		Standard	0.48
	MINI TWIST	Troncated high (2.3)	0.42
		F.27	all versions
	BOEING	Transport A-SS	0.56

Results

Life-times are defined as the number of applied flights to make the crack grow from a minimum to a maximum length both depending on the specimen type and test conditions. Every life-time predictions are compared to the full corresponding test life-times, partial results are not considered. Thus it gives an average effect in prediction- test comparison especially when calculated and experimental crack growth rates differ during a test.

Results under military spectrum are plotted on the classical log diagram of Fig 12. The 42 prediction test ratios range from 0.45 (conservative) to 1.6 (unconservative) with only one result under 0.5. No noticeable trend appears concerning thicknesses.

In a similar manner, results under civil spectrum are shown on the Fig 13. The scattering is larger compared to the one of Fig 12. The 30 prediction test ratios range from 0.4 (with 3 cases lower than 0.5) to 1.8 provided that the strongest unconservative case, 3.3, be neglected. This latter is corresponding to a test under MINITWIST spectrum with high load level and where the life-time was less than two sequences.

Finally the overall result is considered as satisfactory considering in particular simplifications or lack of material data.

CONCLUSION

In the presented work the up-to-date definition of the ONERA model for predicting crack growth under variable loading is completely described. The model uses the evolutive propagation threshold concept in a similar manner than the crack opening one. Besides it is assumed that any loading history can be summarized with the need of two additional internal variables accounting for respectively overload and compressive load effect.

The identification of the model for a given material mainly consists of the knowledge of two experimental functions,  $f_1$  and  $f_2$ , that we consider of great importance.

The model is valid for repeated loading sequence like aeronautical standard spectrum, by introducing a loading parameter connected to the considered loading and representative of it.

Using this model, a comparison between fatigue crack growth life-time predictions and corresponding tests is presented. More of 70 results are reviewed dealing with various conditions : specimen types, alloys, thicknesses, civil and military aircraft spectra, load levels. Neglecting one case, all the prediction-test ratios range between 0.4 (conservative) and 1.8 (unconservative), that is considered as a good result.

## Symbols

C	= material crack growth constant (MPa,m)
e	= specimen thickness (mm.)
KM	= maximum SIF (MPa.m <sup>1/2</sup> )
KMeq	= equivalent max. SIF (MPa.m <sup>1/2</sup> )
KMO	= overload max. SIF (MPa,m <sup>1/2</sup> )
Km	= minimum SIF (MPa,m <sup>1/2</sup> )
Kmeq	= equivalent min. SIF (MPa,m <sup>1/2</sup> )
KS	= propagation threshold SIF (MPa.m <sup>1/2</sup> )
R	= stress ratio or SIF ratio
R <sub>1</sub> <sup>c</sup>	= critical overload ratio , R = 0
R <sub>2</sub> <sup>c</sup>	= critical high-low levels ratio, R = 0
α	= loading parameter
Δa	= crack growth increment (m.)
n	= material crack growth constant
ρ	= length of plastic zone, plane stress case (mm.)
ρ <sub>eq</sub>	= equivalent length of plastic zone, pl. stress case (mm.)
ρ <sub>m</sub>	= mean length of plastic zone (mm.)
ρ <sub>mOL</sub>	= mean length of plastic zone due to overload (mm.)
ρ <sub>OL</sub>	= length of plastic zone due to overload, pl. stress case (mm.)
σ <sub>YS</sub>	= yield stress, 0.2 % offset (MPa)

## References

1. Wheeler, O.E., Journal of Basic Engineering, Vol 94, 1,(1972) 181
2. Willenborg, J.D., Engle, R.M., and Wood, H.A., Report AFFDL-TM-71-1-FBR, (1971).
3. Newman, J.C., Jr., ASTM-STP 748, (1981) 53.
4. Johnson, W.S., ASTM-STP 748, (1981) 85.
5. Rudd, J.L., and Engle, R.M., ASTM-STP 748, (1981) 103.
6. Chang, J.B., Szamossi, M., and Liu, K.W., ASTM-STP 748 (1981) 115.
7. Schijve, J., Report LR-282, Delf University of Technology, (1979).
8. De Koning, A.U., ICAF, Noordwijkerhout, Netherlands, May 1981.
9. Pellas, J., Baudin, G., and Robert, M., ICF4, Waterloo, Canada, June 1977.
10. Elber, W., ASTM-STP 486, (1971) 230.
11. Baudin, G., and Robert, M., ICAF, Noordwijkerhout, Netherlands, May 1981
12. Pellas, J., Baudin, G., and Robert, M., Rech. Aerosp., 3, (1977) 191.
13. Van der Linden, H.H., Report TR 79121L, NLR, (1979).
14. Salvetti, A., Cavallini, G., and Lazzeri, L., Report DA ERO-78-G-107, European Research Office, (1982).
15. Chang, J.B., ASTM-STP 748, (1981) 3.
16. Gunther, C.K., and Goranson, U.G., ICAFMS, Freiburg, Germany, June 1983.
17. Baudin, G., Gateau, M., and Herteman, J.P., Revue de Metallurgie, (1982) 649.

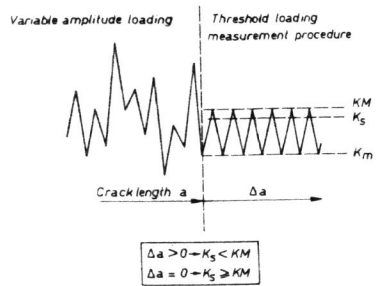


Fig. 1 - Definition of threshold loading measurement procedure

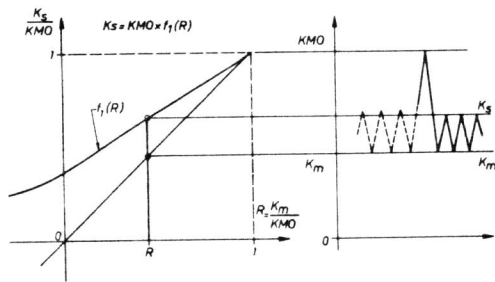


Fig. 2 - Threshold loading measurement after one overload.

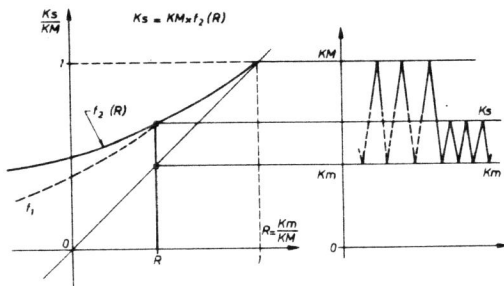


Fig. 3 - Constant amplitude case - Threshold loading measurement.

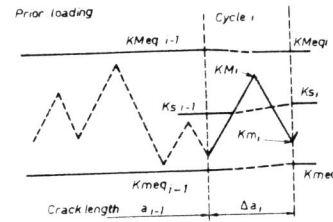


Fig. 4 - The three internal variables used for the description of loading history effect.

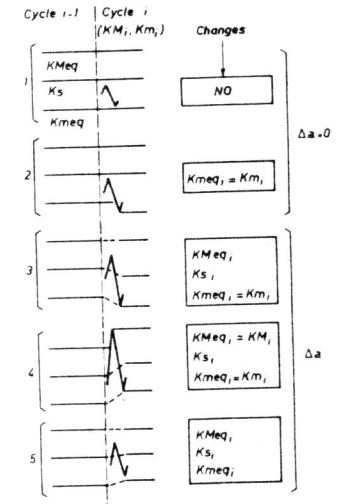


Fig. 5 - The five types of cycle.

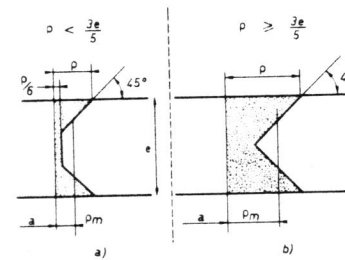
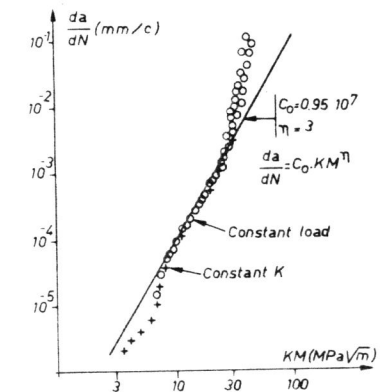


Fig. 6 - Plane strain plane stress transition. Diagram of plastic zone size.

Fig. 7 - Constant amplitude tests. 2024-T3, e = 2mm. Determination of material crack growth constants.



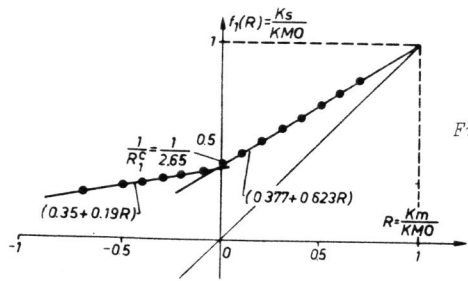


Fig. 8 - One-overload case. Determination of function  $f_1$ . 2024-T3,  $e = 2$  mm.

Fig. 9 - Constant amplitude case. Determination of function  $f_1$ . 2024-T3,  $e = 2$  mm.

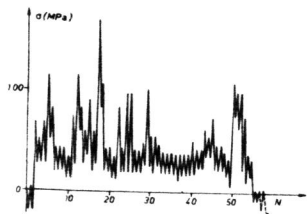
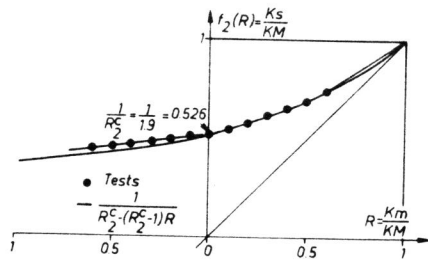


Fig. 10 - Flight type of military aircraft spectrum.

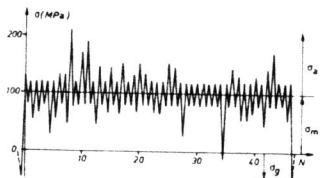


Fig. 11 - Flight type of civil aircraft spectrum.

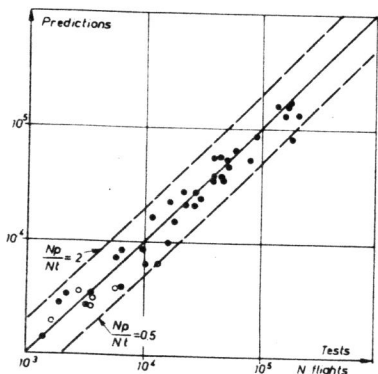


Fig. 12 - Prediction-test life-time comparison for military aircraft spectra.

- thickness  $\leq 2$  mm.
- thickness  $\geq 6.35$  mm.

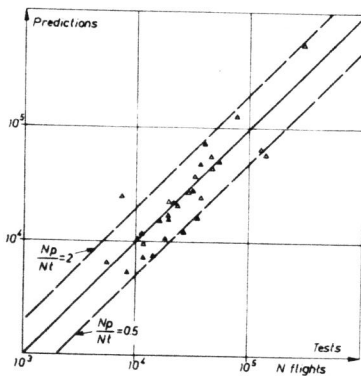


Fig. 13 - Prediction-test life-time comparison for civil aircraft spectra.

- △ thickness  $\leq 2$  mm.
- ▲ thickness  $\geq 8$  mm.